



Beata Krzaczek¹, Natalia Ryłko^{2*}, Paweł Kurtyka²

¹ Pedagogical University of Cracow, ul. Podchorążych 2, 30-084 Krakow, Poland

² Pedagogical University of Cracow, Institute of Technology, ul. Podchorążych 2, 30-084 Krakow, Poland

*Corresponding author. E-mail: nrylko@up.krakow.pl

Received (Otrzymano) 26.03.2018

EFFECTIVE CONDUCTIVITY OF PARTICLE-REINFORCED COMPOSITES WITH CRACKS AT PARTICLE-MATRIX INTERFACE

In the present paper, a new approximate analytical formula for the effective conductivity of 2D dilute composites with poorly conducting circular inclusions and cracks on the interface between the inclusions and the matrix is established. This formula is proved by Maxwell's approach and Keller's identity using advanced complex analysis. The obtained formula is used to determine the effective thermal conductivity of a composite material being an aluminum matrix based on Al-Mg-Si alloy reinforced with Al₂O₃ particles with the average size of about 25 microns and a volume fraction of 20%. The computer simulation results are presented in tables and illustrated by figures. It follows from the derived formulas that cracks reduce the effective heat conductivity about 9% with respect to the material without cracks.

Keywords: effective conductivity, particle-reinforced composite, cracks

EFEKTYWNA PRZEWODNOŚĆ KOMPOZYTÓW WZMOCNIONYCH CZĄSTKAMI Z UWZGLĘDNIENIEM SZCZELIN NA GRANICY CZĄSTKA-OSNOWA

Przedstawiono wzór na efektywną przewodność cieplną kompozytu wzmocnionego kołowymi cząstkami o niskim współczynniku przewodności cieplnej, wyznaczoną z uwzględnieniem szczelin na granicy pomiędzy wtrąceniem a osnową. Wzór był wyprowadzony z wykorzystaniem aproksymacji Maxwella, zaawansowanej analizy zespolonej oraz tożsamości Kellera. Opracowany dwuwymiarowy model oraz wzór zastosowano do teoretycznego wyznaczenia efektywnej przewodności cieplnej kompozytu o osnowie stopu Al-Mg-Si wzmocnionego cząstkami Al₂O₃ o udziale objętościowym wynoszącym 20% i średniej wielkości na poziomie 25. Kompozyt został poddany ścisłaniu osiowemu, w wyniku którego w jego strukturze pojawił się szereg pęknięć, szczelin. Z analizy obrazu materiału po ścisłaniu uzyskano dane niezbędne do dalszych obliczeń: numer cząstki, udział powierzchniowy cząstki, rozpiętość kąta (w stopniach). Wykonano obliczenia efektywnej przewodności według wyprowadzonego wzoru dla przypadków rzeczywistego oraz modelowych. Z analizy wyników obliczeń efektywnej przewodności cieplnej kompozytu Al-Mg-Si/Al₂O₃ wynika, że obecność szczelin w badanym materiale kompozytowym obniża jego właściwości przewodzenia ciepła około 9% w stosunku do materiału bez pęknięć. Dodatkowe symulacje pokazują znaczący wpływ pęknięć na właściwości przewodzenia ciepła. W granicznym przypadku dodania szczelin o rozpiętości 90° w Modelu 6 obniża je do poziomu 85% materiału bez pęknięć. Otrzymane wyniki pokazują dynamiczne zmiany efektywnych właściwości kompozytu następujące w wyniku zwiększenia kąta rozpiętości szczelin/zwiększenia ich liczby. Uzyskany wzór może być stosowany we wszystkich dziedzinach inżynierii materiałowej, związanej z określaniem efektywnych właściwości cieplnych, elektrycznych etc. materiałów kompozytowych z uwzględnieniem pęknięć, pojawiających się na granicach fazy wzmacniającej.

Słowa kluczowe: efektywna przewodność, kompozyty wzmocnione cząstkami, szczeliny

INTRODUCTION

The extensive development of high-tech industries (automotive, aerospace, etc.) sets very high demands on the choice of engineering materials. The use of traditional materials has limited possibilities, hence, there is a need to look for innovative materials including composites, hybrid composites, metamaterials, smart materials, etc. [1-6].

The above mentioned factors are the driving force in promoting research in the field of composite materials, both theoretical [7-9] and experimental [10-13].

Experimental work also stimulates the development of theoretical investigation based on mathematical models in order to predict the effective properties of composite materials at the design stage [14-16]. The well-known historical formulas and models [17-19] are still being applied by engineers for preliminary estimates of composite material properties. However, their applications are limited by dilute and regular composites [20] without cracks/porous/voids etc. [21]. The latter issue plays a key role in assessing the material properties [20, 22]. Damage in the process of manufac-

turing [23-25], joining [26, 27], modification [28] and material exploitation have a significant influence on the effective properties of material and as a consequence, on the possibilities of their use. The arising material defects considerably impact the effective properties of materials, which has been proven by numerous experimental results [11, 22, 29] as well as by theoretical calculations based on standard equations [30-32]. The results obtained by such methods do not present a full picture and they require further investigation, especially in the area of advanced models developed in [33, 34].

In the majority of studies concerning the effective properties of composites with cracks numerical simulations or statistical methods have been applied [11, 20, 21]. In addition, numerous among the above mentioned studies were based on models with a uniform imperfect interface instead of cracks. In recent years, symbolic computations by means of Mathematica and Maple have been applied to this problem. An analytical formula for the effective conductivity of a two-dimensional composite with circular inclusions and cracks that arose on the surface between the inclusions and the matrix was presented for the first time in [35]. This approach yields the effective thermal conductivity of the Al-Mg-Si/Al₂O₃/20p composite including cracks.

MAXWELL APPROACH

Let us consider the matrix-inclusion type composite with perfect interfacial bonds between the inclusions and the surrounding matrix. Let inclusion phase U_1 be a disk of radius R_0 with the center at the origin. Let λ denote the conductivity of the inclusions and the conductivity of the matrix domain U^- be normalized to unity. Introduce complex variables $z = x + iy$, $i^2 = -1$. Then, the thermal conductivity can be represented by the form

$$\lambda(x, y) \equiv \lambda(z) = \begin{cases} 1 & \text{for } |z| > R_0, \\ \lambda & \text{for } |z| < R_0. \end{cases} \quad (1)$$

Temperature distribution $T_1(z) \equiv T_1(x, y)$ in U_1 and $T(z) \equiv T(x, y)$ in U^- satisfies the Laplace equation

$$\nabla^2 T_1(x, y) = 0, \quad (x, y) \in U_1, \quad \nabla^2 T(x, y) = 0, \quad (x, y) \in U^- \quad (2)$$

And asymptotic conditions at infinity

$$T(x, y) \sim x, \quad \text{when } |(x, y)| \rightarrow \infty. \quad (3)$$

The perfect contact condition between the inclusion and matrix takes the form [36, 37]

$$T = T_1, \quad \frac{\partial T}{\partial n} = \lambda \frac{\partial T_1}{\partial n} \quad \text{on } |z| = R_0, \quad (4)$$

where $\frac{\partial}{\partial n}$ means a normal derivative on $|z| = R_0$.

The harmonic functions can be expressed in terms of the complex potentials

$$T(z) = Re\Phi(z), \quad T_1(z) = \frac{2}{\lambda+1} Re\Phi_1(z). \quad (5)$$

Here, $\Phi_1(z)$ is analytic in $|z| < R_0$ and $\Phi(z)$ is analytic in $|z| > R_0$ except at infinity, where $\Phi(z) \sim z$.

Problem (4) can be written as the \mathbb{R} -linear problem for complex potentials in the following form

$$\Phi(z) = \Phi_1(z) - \rho \overline{\Phi_1(z)} \quad \text{on } |z| = R_0, \quad (6)$$

where $\rho = \frac{\lambda-1}{\lambda+1}$ is the contrast parameter. The \mathbb{R} -linear problem has the following solution [36]

$$\Phi(z) = z + c - \rho \bar{c} - \frac{\rho R_0^2}{z}, \quad \Phi_1(z) = z + c, \quad (7)$$

where c is an arbitrary constant.

Suppose that N small non-overlapping disks are located inside a large disk $|z| < R_0$. Let the conductivity of the large disk be equal to $\lambda = \lambda_e$.

The coefficient of $-z^{-1}$ of a complex potential is called the dipole moment of the potential [38].

Hence, the dipole moment of $\Phi(z)$ is equal to $\rho_e R_0^2$, where ρ_e is the contrast parameter given by the formula

$$\rho_e = \frac{\lambda_e - 1}{\lambda_e + 1}. \quad (8)$$

For perfect conductors $\rho = 1$, hence the dipole moment of each perfectly conducting small disk is equal to r_0^2 . The sum of the dipole moments of the small disks is equal to Nr_0^2 . We set the sum of the dipole moments of the small disks equal to the total dipole moment of the homogenized material

$$\rho_e R_0^2 = N\rho r_0^2. \quad (9)$$

Let us recall, Clausius-Mossotti's classic formula for effective conductivity, given by

$$\lambda_e \approx \frac{1 + \rho\nu}{1 - \rho\nu}. \quad (10)$$

Using a formula (8), (9) and (10) with $\rho = 1$, we conclude that for a sufficiently large number of small non-overlapping disks N , concentration ν can be approximated by $N(r_0/R_0)^2$. The theoretical background of the methods and its validity were discussed in [39, 40].

Following the previous section, we will extend Maxwell's approach when different parts of the interface combine ideal contact and isolation. Suppose that N small disks are located inside large disk $|z| < R_0$, according to the above assumptions. The dipole moment of a large disk of $\Phi(z)$ is equal to $\rho_e R_0^2$.

Now we apply the Maxwell approach to small disks D_k ($k = 1, 2, \dots, N$) of radius r_0 embedded in the matrix. Let M_k denote the dipole moment of complex potential $\varphi(z)$ for a small disk. It is equal to coefficient φ_1 of $-z^{-1}$ in the Laurent expansion. The total dipole moment becomes

$$\rho_e R_0^2 = \sum_{k=1}^N M_k. \quad (11)$$

Let all N inclusions be divided into n representative classes. Then, (11) becomes

$$\rho_e R_0^2 = \sum_{i=1}^n n_i M_i, \quad (12)$$

where n stands for the number of classes and n_i for the frequency of the i -th class.

EFFECTIVE CONDUCTIVITY

In the present paper, a new approximate analytical formula for the effective conductivity of 2D dilute composites with poorly conducting circular inclusions and cracks on the interface between the inclusions and the matrix is deduced.

First, we describe a formula obtained in [35], where perfect conductors of conductivity λ_1 were embedded in a matrix of conductivity $\lambda \ll \lambda_1$. On the boundary of an inclusion, the size of insulating crack ψ was determined by the central angle which spans the boundary fracture. On the remaining part of the interface, the perfect contact conditions were given, i.e. the continuity of the temperature and of the normal heat fluxes from both sides of the interface (see Fig. 1).

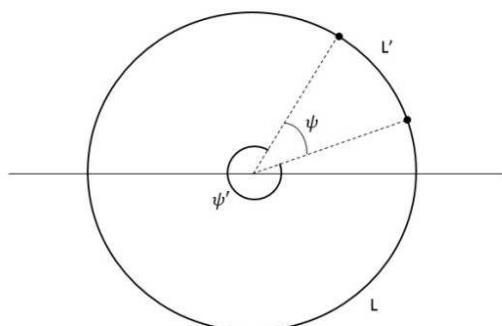


Fig. 1. Circular inclusions with interfacial fracture L' of angle length ψ
Rys. 1. Wtrącenie kołowe ze szczeliną na brzegu L' o wymiarze kątowym ψ mierzonym w radianach

It was assumed that all the inclusions were randomly located in the matrix. Let k denote the number of inclusions. The corresponding spanning angles ψ_k have an angle orientation. It was assumed that these orientations were uniformly distributed in the segment $(0, 2\pi)$. Therefore, the considered composites on the macroscale were isotropic and described by scalar effective conductivity λ'_e . It was calculated by the following equation:

$$\lambda'_e = \lambda \frac{1 + \nu \langle \cos \frac{\psi}{2} \rangle}{1 - \nu \langle \cos \frac{\psi}{2} \rangle}. \quad (13)$$

Here, $\langle \cos \frac{\psi}{2} \rangle$ means the statistical averaged value of the cosines of the spanning angles and ν stands for the concentration of inclusions. The formula was proved for dilute composites in limit case $\lambda_1 \rightarrow \infty$ by means of Maxwell's approach [36].

The case that will be considered below is geometrically identical to the previous one, with the exception of the relation between conductivity of inclusions λ and matrix conductivity λ_1 which in the present case holds as $\lambda_1 \gg \lambda$. The latter condition is opposite to the case discussed in [35], hence direct application of formula (13) will be incorrect.

Keller's identity [40] takes place for 2D composites when the constituents are replaced by each other

$$\lambda'_e \lambda_e = \lambda \lambda_1. \quad (14)$$

Here, λ'_e denotes the effective conductivity of composites corresponding to [35] when the conductivity of the inclusions is much greater than the conductivity of the matrix, i.e., $\lambda_1 \gg \lambda$.

It is impossible to directly apply Keller's identity because it was deduced under perfect contact conditions between the composite components/phases. Now, we have to take into account the insulating cracks on the inclusion boundaries. The main fact used by Keller [40] was the orthogonality of the temperature level lines and the flux streamlines. It was also noted that replacing conductivity λ by resistivity λ^{-1} is equivalent to replacing by each other the materials occupying the inclusions and matrix domains. A similar interpretation takes place in complex analysis when the level lines of the real and imaginary parts of the analytic functions are orthogonal. It worth adding that the real and imaginary parts of the analytic functions satisfy Laplace's equation governing 2D steady heat conduction [36]. Therefore, in the framework of dual formalism, insulating cracks have to be replaced by perfect line conductors. Therefore, Keller's identity (14) can be extended to 2D composites when the original composite contains cracks and the dual composite contains line perfect conductors instead of cracks.

Consider the following conductivity scales $\lambda_{lines} \gg \lambda_1 \gg \lambda$ in a composite with high conducting lines of conductivity λ_{lines} and with the high ratio $\frac{\lambda_1}{\lambda}$ of matrix to inclusion conductivities. It follows from (13) and (14) that the effective conductivity of the considered composite holds

$$\lambda'_e = \lambda_1 \frac{1 + \nu \langle \cos \frac{\psi'}{2} \rangle}{1 - \nu \langle \cos \frac{\psi'}{2} \rangle}, \quad (15)$$

where ψ' stands for the spanning angle of the perfectly conducting lines on the boundary of inclusions L' . The remaining part of the interface denoted by L has a spanning angle of ideal contact conditions between the inclusions and matrix $\psi = 2\pi - \psi'$ (see Fig. 1). This formula is deduced under the condition that conductivity λ_{lines} of the part of boundary L' tends to infinity. Substituting $\psi' = 2\pi$ into (15) yields $\frac{1+\nu}{1-\nu}$ instead of 1 in the case $\lambda_1 \sim \lambda_{lines}$. It can be noted that $\lambda_e = \lambda_1$ when $\psi' = \pi$. This enables us to rescale the conductivity via angle ψ' and instead of (15) to take

$$\lambda_e = \lambda_1 \frac{1 + \nu \langle \cos \frac{\psi'}{4} \rangle}{1 - \nu \langle \cos \frac{\psi'}{4} \rangle} \quad (16)$$

to describe case $\lambda_1 \sim \lambda_{lines}$. Such rescaling means linear correction of the conductivity along L' .

Let T denote the temperature distribution in the composite. Then, the normal fluxes inside and outside the inclusion coincide

$$\lambda \frac{\partial T^+}{\partial n} = \lambda_1 \frac{\partial T^-}{\partial n} \quad \text{on } L. \quad (17)$$

Because of inequality $\lambda_1 \gg \lambda$ in the limit case (17) becomes

$$\frac{\partial T^+}{\partial n} = 0 \quad \text{on } L. \quad (18)$$

This means insulation along the considered part of the boundary, hence, ψ yields the spanning angle of insulation. Substituting $\psi' = 2\pi - \psi$ into (16) implies the following formula

$$\lambda_e = \lambda_1 \frac{1 + \nu \langle \sin \frac{\psi}{4} \rangle}{1 - \nu \langle \sin \frac{\psi}{4} \rangle} \quad (19)$$

Following Section *Maxwell approach*, we use the dipole approach and extend the latter formula to polydispersed inclusions

$$\lambda_e = \lambda_1 \frac{1 + \sum_{i=1}^n v_i \langle \sin \frac{\psi_i}{4} \rangle}{1 - \sum_{i=1}^n v_i \langle \sin \frac{\psi_i}{4} \rangle} \quad (20)$$

where n is the number of inclusions phases, v_i the concentration of the i -th component, ψ_i the spanning angle of insulation of the i -th component.

CALCULATIONS

In this section the theory described above will be used to determine the effective properties of the Al-Mg-Si/Al₂O₃ composite with a reinforcing phase concentration of about 20% (Fig. 2).

The composite was subjected to axial compression in which a number of cracks and gaps arose in its structure. We obtain the data necessary for further calculations - the number of particles, the particle fraction areas, the crack spanning angles (in degrees) from the image analysis of Figure 3. The crack formation in the composite structure as a result of the plastic deformation process can be considered as a dynamic process of the external load changing in time. Therefore, in order to obtain the necessary data to estimate the influence of crack propagation on the effective properties of the composites, six additional models are built on the basis of the actual image of the microstructure (Fig. 3). Models 1-3 are created as a result of the linear reduction of the angle of the slit gap to the levels of 1/3, 1/2 and 2/3 of the real data, respectively. In models 4-6, the slits are introduced artificially (they are not presented in the microstructure image) with a span of 30, 60, 90, respectively.

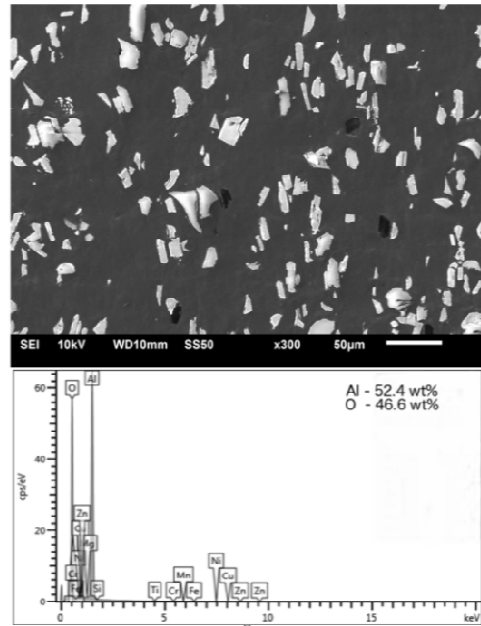


Fig. 2. Initial microstructure of Al-Mg-Si/Al₂O₃/20p composite with EDS analysis results of its major structural constituent Al₂O₃

Rys. 2. Obraz mikrostruktury kompozytu Al-Mg-Si/Al₂O₃/20p z analizą EDS cząstek wzmocnienia

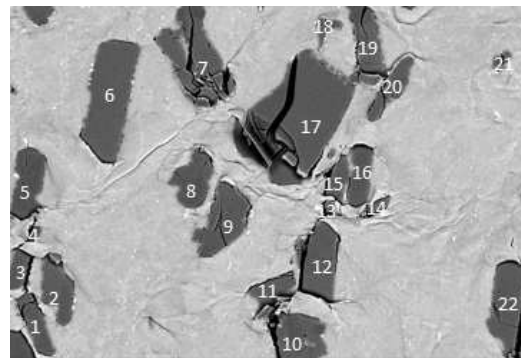


Fig. 3. Microstructure of Al-Mg-Si/Al₂O₃/20p composite after plastic deformation with visible cracks

Rys. 3. Mikrostruktura kompozytu Al-Mg-Si/Al₂O₃/20p po deformacji z widocznymi szczelinami

The sets of real and model data (description in further part of this paper) are shown in Table 1.

The data from Figure 3 are in the column entitled *REAL*, in the next ones the data is changed as follows:

- *Model 1* - the crack spanning angles are reduced to the level $\frac{1}{3} \cdot (\text{real data})$;
- *Model 2* - as above to the level $\frac{1}{2} \cdot (\text{real data})$;
- *Model 3* - as above to the level $\frac{2}{3} \cdot (\text{real data})$;
- *Model 4* - in relation to the *REAL* column, the data is changed by adding cracks with a span angle equal to 30° at the particle-matrix boundary where no cracks occurred before;
- *Model 5* - as above with the angle of 60°;
- *Model 6* - as above with the angle of 90°.

Calculations were made for effective conductivity of the considered composite without cracks using equation (20) for the real cases and for the models mentioned

above. For the purpose of comparison of the obtained results, the effective conductivity of the considered composite without cracks is calculated by the Clausius-Mossotti (Maxwell) model

$$\lambda_e \approx \lambda_1 \frac{1+\rho v}{1-\rho v} \tag{21}$$

The obtained results for the calculated heat effective conductivity are shown in Table 2.

TABLE 1. Sets of real and model data for further calculations on basis of Figure 3

TABELA 1. Zestawienie modelowych i rzeczywistych danych do obliczeń na podstawie rysunku 3

N	Fraction area	Crack spanning angle (in degrees)						
		Real	Model 1	Model 2	Model 3	Model 4	Model 5	Model 6
1	0.007	46.69	15.56	23.35	31.13	46.69	46.69	46.69
2	0.009	-	-	-	-	30.00	60.00	90.00
3	0.004	110.25	36.75	55.13	73.50	110.25	110.25	110.25
4	0.001	111.45	37.15	55.73	74.30	111.45	111.45	111.45
5	0.010	41.57	13.86	20.79	27.71	41.57	41.57	41.57
6	0.025	34.91	11.64	17.46	23.27	34.91	34.91	34.91
7	0.025	-	-	-	-	30.00	60.00	90.00
8	0.009	45.66	15.22	22.83	30.44	45.66	45.66	45.66
9	0.015	52.89	17.63	26.45	35.26	52.89	52.89	52.89
10	0.012	97.08	32.36	48.54	64.72	97.08	97.08	97.08
11	0.007	117.71	39.24	58.86	78.47	117.71	117.71	117.71
12	0.014	145.04	48.35	72.52	96.69	145.04	145.04	145.04
13	0.001	79.02	26.34	39.51	52.68	79.02	79.02	79.02
14	0.002	56.93	18.98	28.47	37.95	56.93	56.93	56.93
15	0.005	108.78	36.26	54.39	72.52	108.78	108.78	108.78
16	0.007	53.40	17.80	26.70	35.60	53.40	53.40	53.40
17	0.053	-	-	-	-	30.00	60.00	90.00
18	0.002	-	-	-	-	30.00	60.00	90.00
19	0.011	123.42	41.14	61.71	82.28	123.42	123.42	123.42
20	0.007	-	-	-	-	30.00	60.00	90.00
21	0.002	-	-	-	-	30.00	60.00	90.00
22	0.018	45.18	15.06	22.59	30.12	45.18	45.18	45.18

TABLE 2. Calculated effective conductivity λ
TABELA 2. Zestawienie obliczonych wartości efektywnej przewodności λ

Model	λ
Real	0.913
Model 1	0.969
Model 2	0.954
Model 3	0.940
Model 4	0.889
Model 5	0.867
Model 6	0.845

The obtained results are displayed in a bar chart in Figure 4 where column 0 on the OX axis corresponds to the effective conductivity normalized to unity of the composite without cracks.

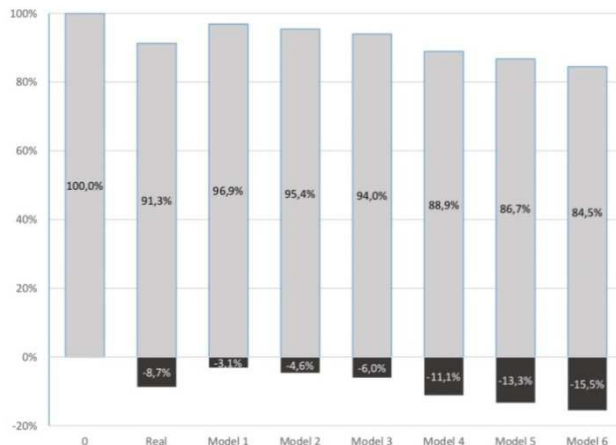


Fig. 4. Calculated effective conductivity λ

Rys. 4. Zestawienie obliczonych wartości efektywnej przewodności λ

The parts of the column under the OX axis correspond to the losses of the effective heat conductivity because of the presence of cracks. The results are predictable - the presence of cracks decreases the value of λ. The decrease of λ holds 8.7% for the real composite material with cracks calculated with formula (20). The decrease in the value of λ and the angle of the cracks span indicates a non-linear relation between the calculations and the performed changes.

CONCLUSIONS

Formula (20) applied to the Al-Mg-Si/Al₂O₃ composite demonstrates that the presence of cracks in the examined composite material decreases its ability to conduct heat by 8.7% in relation to the material without cracks. Furthermore, the simulations show a significant influence of the cracks on the heat conduction, and in the boundary case, adding cracks with the spread of 90° in Model 6 leads to a decrease of about 16% in relation to the material without the cracks.

The dynamics changes in effective properties that occur as a result of the defects increase in the composite are observed. It should be mentioned that the received formula can be adapted for all fields of materials engineering associated with determining the effective heat, electric etc. properties of composite materials with cracks appearing on boundaries of the reinforcing phase.

Acknowledgements

Partial financing of this research was provided by statutory research funds of the Faculty of Mathematics, Physics and Technical Science, Pedagogical University of Krakow, Poland.

REFERENCES

[1] Agarwal B.D., Broutman L.J., Chandrashekhara K., Analysis and Performance of fiber composites, Wiley, USA, 2006.
[2] Formanek B., Józwiak S., Szczucka-Lasota B., Dolata-Grosz A., Bojar Z., Intermetallic alloys with ceramic parti-

- cles and technological concept for high loaded materials, *Journal of Materials Processing Technology* 2005, 162, 46-51.
- [1] Agarwal B.D., Broutman L.J., Chandrashekhara K., *Analysis and Performance of fiber composites*, Wiley, USA, 2006.
 - [2] Formanek B., Józwiak S., Szczucka-Lasota B., Dolata-Grosz A., Bojar Z., *Intermetallic alloys with ceramic particles and technological concept for high loaded materials*, *Journal of Materials Processing Technology* 2005, 162, 46-51.
 - [3] Broutman L.J., Krock R.H., *Composite Materials*, Academic Press, New York and London 1974.
 - [4] Dolata-Grosz A., Śleziona J., Formanek B., Wieczorek J., Al.-FeAl-TiAl-Al₂O₃ composite with hybrid reinforcement, *Journal of Materials Processing Technology* 2005, 162, 33-38.
 - [5] Sobczak J.J., Drenchev L.B., *Prace studialne nad teoretycznymi i praktycznymi aspektami projektowania materiałów lżejszych od powietrza*, *Prace Instytutu Odlewnictwa* 2011, 51(4), 5-30.
 - [6] Dolata A., Dyzia M., Boczek S., Influence of the Sr and Mg alloying additions on the bonding between matrix and reinforcing particles in the AlSi7Mg/SiC-Cg hybrid composite, *Archives of Metallurgy and Materials* 2016, 61, 651-656.
 - [7] Czaplą R., Nawalaniec W., Mityushev V., Effective conductivity of random two-dimensional composites with circular non-overlapping inclusions, *Comp. Materials Sci.* 2012, 6, 118-126.
 - [8] Drygaś P., Mityushev V., Effective elastic properties of random two-dimensional composites, *Int. J. Solids* 2016, 97-98, 543-553.
 - [9] Kurtyka P., Rylko N., Quantitative analysis of the particles distributions in reinforced composites, *Composite Structure* 2017, 182, 412-419.
 - [10] Chen G.M., Teng J.G., Finite-element modeling of intermediate crack debonding in FRP-plated RC beams, *Journal of Composites for Construction* 2011, 15.
 - [11] Teng J.G., Smith S.T., Yao J., Chen J.F., Intermediate crack-induced debonding in RC beams and slabs, *Construction and Building Materials* 2003, 17, 447-462.
 - [12] Zohdi I.T., *Encyclopedia of Computational Mechanics*, Vol. Solids and Structures, Chap. Homogenization Methods and Multiscale Modeling, Wiley 2004, 407-430.
 - [13] Rylko N., Edge effects for heat flux in fibrous composites, *Computers & Mathematics with Applications* 2015, 70, 2283-2291.
 - [14] Batchelor G.K., Transport properties of two-phases materials with random structure, *A. Rev. Fluid Mech.* 1974, 227-255.
 - [15] Bensoussan A., Lions J.L., Papanicolaou G., *Asymptotic Analysis for Periodic Structures*, AMS Chelsea Publishing, Rhode Island 2010.
 - [16] Kolodziej J.A., Streck T., Analytical approximations of the shape factors for conductive heat flow in circular and regular polygonal cross-sections, *Int. J. Heat Mass Transfer* 2001, 44, 999-1012.
 - [17] Einstein A., Eine neue Bestimmung der Moleküldimensionen, *Ann. Phys.* 1905, 19, 289-306.
 - [18] Maxwell J.C., *A Treatise on Electricity and Magnetism*, Volume I, Clarendon Press, Oxford 1873.
 - [19] Rayleigh J.W., On the influence of obstacles arranged in rectangular order upon the properties of a medium, *Phil. Mag.* 1892, 481-491.
 - [20] Sun R., Seviliano E., Perera R., A discrete spectral model for intermediate crack debonding in FRP-strengthened RC beams, *Composites Part B: Engineering* 2015, 69, 562-575.
 - [21] Li W., Jiang Z., Yang Z., *Crack Extension and Possibility of Debonding in Encapsulation-Based Self-Healing Materials*, Basel 2017.
 - [22] Ombres L., Prediction of intermediate crack debonding failure in FRP-strengthened reinforced concrete beams, *Composite Structures* 2010, 92, 322-329.
 - [23] Jahedi M., Paydar M.H., Three-dimensional finite element analysis of torsion extrusion (TE) as an SPD process, *Materials Science and Engineering* 2011, 528, 8742-8749.
 - [24] Azarniya A., Hosseini H.R.M., A new method for fabrication of in situ Al/Al₃Ti-Al₂O₃ nanocomposites based on thermal decomposition of nanostructured tialite, *Journal of Alloys and Compounds* 2015, 643, 64-73.
 - [25] Blaz L., Lobry P., Zygmunt-Kiper M., Koziel J., Wloch G., Dymek S., Strain rate sensitivity of Al.-based composites reinforced with MnO₂ additions, *Journal of Alloys and Compounds* 2015, 619, 9, 652-658.
 - [26] Rams B., Pietras A., Mroczka K., Friction stir welding of elements made of case aluminum alloys, *Archives of Metallurgy and Materials* 2014, 59, 385-392.
 - [27] Mroczka K., Characteristics of AlSi9Mg/2017A aluminum alloys friction stir welded with offset welding line and root-side heating, *Archives of Metallurgy and Materials* 2014, 59, 1293-1299.
 - [28] Blaz L., Sugamata M., Kaneko J., Sobota J., Wloch G., Bochniak W., Kula A., Structure and properties of 6061+26 mass % Si aluminum alloy produced via coupled rapid solidification and KOB0-extrusion of powder, *Journal of Materials Processing Technology* 2009, 209(9), 4329-4336.
 - [29] Fu B., Chen G.M., Teng J.G., Mitigation of intermediate crack debonding in FRP-plated RC beams using FRP U-jackets, *Composite Structures* 2017, 176, 883-897.
 - [30] Hatta H., Taya M., Effective thermal conductivity of a misoriented short fiber composite, *J. Appl. Phys.* 1985, 58, 2478-2486.
 - [31] Benveniste Y., Miloh T., The effective conductivity of composites with imperfect thermal contact at constituent interfaces, *Int. J. Eng. Sci.* 1986, 24, 1537-1552.
 - [32] Schulgasser K., Concerning the effective transverse conductivity of a two-dimensional two-phase material, *Int. J. Heat Mass Transfer* 1977, 20, 1273-1280.
 - [33] Rylko N., Effective anti-plane properties of piezoelectric fibrous composites, *Acta Mechanica* 2013, 224, 2719-2734.
 - [34] Mityushev V., Rylko N., Bryła M., Conductivity of two-dimensional composites with randomly distributed elliptical inclusions, *Zeitschrift für Angewandte Mathematik und Mechanik* 2017.
 - [35] Rylko N., Krzaczek B., Mityushev V., Conductivity of fibre composites with fractures on the boundary of inclusions, *Multiscale Model. Simul.* 2013, 11, 152-161.
 - [36] Gluzman S., Mityushev V., Nawalaniec W., *Computational Analysis of Structured Media*, Elsevier, Amsterdam 2017.
 - [37] Mityushev V., Pesetskaya E., Rogosin S., Analytical Methods for Heat Conduction in Composites and Porous Media, in *Cellular and Porous Materials: Thermal Properties Simulation and Prediction*, A. Ochsner, G.E. Murch, M.J. S. de Lemos, eds., Wiley 2008, 121-164.
 - [38] Movchan A.B., Movchan N.V., Poulton C.G., *Asymptotic Models of Fields in Dilute and Densely Packed Composites*, Imperial College Press, London 2002.
 - [39] Mityushev V., Rylko N., Maxwell's approach to effective conductivity and its limitations, *The Quarterly Journal of Mechanics and Applied Mathematics* 2013, 66, 2, 241-251.
 - [40] Keller J.B., Conductivity of a medium containing a dense array of perfectly conducting spheres or cylinders or non-conducting cylinders, *J. Appl. Phys.* 1963, 34, 991-993.